Cancer Science
Japanese Cancer Association JCA
Open Access

Downregulation of *TBXAS1* in an iron-induced malignant mesothelioma model

Daisuke Minami,[1] Nagio Takigawa,[2] Yuka Kato,[3] Kenichiro Kudo,[3] Hideko Isozaki,[3] Shinsuke Hashida,[4,5] Daijiro Harada,[1] Nobuaki Ochi,[2] Masanori Fujii,[1] Toshio Kubo,[1] Kadoaki Ohashi,[1] Akiko Sato,[1] Takehiro Tanaka,[6] Katsuyuki Hotta,[1] Masahiro Tabata,[1] Shinichi Toyooka,[4,5] Mitsune Tanimoto[3] and Katsuyuki Kiura[1]

[1]Department of Hematology, Oncology and Respiratory Medicine, Okayama University Hospital, Okayama; [2]Department of General Internal Medicine, Kawasaki Medical School, Okayama; [3]Department of Hematology, Oncology and Respiratory Medicine, Okayama University Graduate School of Medicine, Dentistry and Pharmaceutical Sciences, Okayama; Departments of [4]Thoracic, Breast and Endocrinological Surgery; [5]Clinical Genomic Medicine; [6]Pathology, Okayama University Hospital, Okayama, Japan

Key words

Asbestos, carcinogenesis, iron, malignant mesothelioma, TBXAS1

Correspondence

Daisuke Minami, Department of Hematology, Oncology, and Respiratory Medicine, Okayama University Hospital, Okayama 700-8558, Japan.
Tel: 086-223-7151; Fax: 086-235-7636;
E-mail: d-minami@bj8.so-net.ne.jp

Funding information

Ministry of Education, Culture, Sports, Science, and Technology, Japan (23659432). Okayama University Center of Excellence Strategic Research Foundation Grant-aided Project for Private Universities Ministry of Education, Culture, Sport, Science, and Technology, Japan Grant-in-Aid from Novartis Pharma K.K, Japan

Received March 12, 2015; Revised July 13, 2015; Accepted July 18, 2015

Cancer Sci **106** (2015) 1296–1302

doi: 10.1111/cas.12752

Malignant mesothelioma is an aggressive and therapy-resistant neoplasm arising from mesothelial cells. Evidence suggests that the major pathology associated with asbestos-induced mesothelioma is local iron overload. In the present study, we induced iron-induced mesothelioma in rats based on previous reports. Ten Wistar rats were given ferric saccharate and nitrilotriacetate i.p. for 5 days a week. Five of the ten rats exhibited widespread mesotheliomas in the peritoneum and tunica vaginalis. The tumor cells showed positive immunostaining for calretinin, wilms tumor-1, podoplanin and the oxidative DNA marker 8-hydroxy-2′-deoxyguanosine. In three of the five rats with mesothelioma, array-based comparative genomic hybridization analysis identified a common chromosomal deletion mapped to the chromosomal 4q31 locus, which encompasses the *TBXAS1* gene. Downregulation of the *TBXAS1* gene was confirmed using quantitative PCR. *TBXAS1* gene expression was also reduced in three of four human malignant pleural mesothelioma cell lines compared with normal bronchial epithelial cells. Immunohistochemistry revealed that *TBXAS1* expression was weakly positive and positive in five and three out of eight human malignant mesothelioma samples, respectively. In conclusion, *TBXAS1* gene expression was downregulated in rats with iron-induced mesothelioma. The relationship between iron overload and *TBXAS1* downregulation should be pursued further.

Malignant mesothelioma is an aggressive and therapy-resistant neoplasm arising from mesothelial cells.[1] The median survival time of advanced cases is <12 months, and most patients die within 10–17 months of their initial symptom onset.[2] Furthermore, the incidence of malignant mesothelioma in Japan is expected to peak in 2025, and >100 000 individuals will suffer from the disease in the next 40 years.[3] There is a significant relationship between asbestos exposure and malignant mesothelioma.[4] Additional evidence suggests that local iron overload is a major pathology associated with asbestos-induced malignant mesothelioma.[5]

Iron is the most abundant heavy metal in mammals. It is an essential element and a critical component of molecules involved in energy production, the cell cycle and intermediate metabolism.[6] Nevertheless, iron can be toxic as a consequence of increased oxidative stress[7] and was found to be carcinogenic in experimental models.[8] The intramuscular injection of iron dextran, a colloidal form of iron, induced sarcoma in rats.[9] In an iron-induced mesothelioma model, Okada *et al.*[10] demonstrate that iron plays a major role in catalyzing free radical production, leading to lipid peroxidation and DNA damage, and that iron deposits in the peritoneum caused neoplastic changes in the mesothelium. In the present study, we first confirmed the iron-induced mesothelioma model of those authors and then examined the entire rat genome using array-based comparative genomic hybridization (CGH). Finally, we evaluated whether the results of the CGH analysis could be extrapolated to human mesothelioma cell lines and clinical samples.

Materials and Methods

Ferric nitrilotriacetate-induced malignant peritoneal mesothelioma. Male Wistar rats were purchased from Charles River Development Japan (Yokohama, Japan). The animal experiment committee of the Department of Animal Resources, Okayama University Advanced Science Research approved the study protocol. The Fe-NTA-induced malignant peritoneal mesothelioma model was generated in 14 rats using a method reported previously.[10] There were two control groups, the physiological saline solution (PSS; group 1, $n = 2$) and NTA (group 2, $n = 2$) groups, while the experimental group (group 3, $n = 10$) was administered both NTA and ferric saccharate ($n = 10$). The NTA solution was pre-

pared by dissolving nitrilotriacetic acid disodium salt (Nacalai Tesque, Kyoto, Japan) in PSS, and the pH was adjusted to approximately 7.0 using sodium bicarbonate. Ferric saccharate solution (Fesin, Nichi-Iko Pharmaceutical, Toyama, Japan) was diluted in 5% glucose solution. PSS (0.5 mL) was administered i.p. to rats in group 1 for 5 days a week for 3 months. The rats in groups 2 and 3 were administered 83.5 mg/kg/day NTA i.p. for 5 days a week for 5 months. The dose of ferric saccharate given to group 3 was 5 mg iron/kg bodyweight/day i.p. for 5 days a week for 3 months. All animals were killed 2 years later. Samples were then harvested, stained with H&E and visualized using light microscopy.

Cell lines and clinical samples. Four malignant mesothelioma cell lines (H2052, H28, MSTO-211H and H290) were used, and a human bronchial epithelial cell line (Met5A) was established from non-malignant human bronchial cells.[11] H2052 and H290 cell lines are of epithelial type, H28 is of sarcomatoid type, and MSTO-211H is of biphasic type. The H2052, H28 and H290 cell lines were a generous gift from Dr Adi F. Gazdar (University of Texas Southwestern Medical Center, Dallas, TX, USA). The Met5A and MSTO-211H cell lines were purchased from the American Type Culture Collection (Manassas, VA, USA). Cells were cultured at 37°C in 5% CO_2 in RPMI-1640 supplemented with 10% heat-inactivated FBS. Eight patients with malignant mesothelioma and one patient with non-malignant pleural thickening (mesothelial hyperplasia) who had undergone surgery at Okayama University Hospital were enrolled in the study. The Institutional Ethics Committee of Okayama University Hospital approved the study protocol. The malignant mesothelioma patients included seven men and one woman; the mean age was 65 years. Histologically, two tumors were epithelioid, three were biphasic and three were sarcomatoid.

Antibodies. Anti-carcinoembryonic antigen (CEA) rabbit polyclonal antibodies (ab33562), anti-wilms tumor-1 rabbit polyclonal antibodies (ab96792) and anti-EpCAM mouse monoclonal antibodies (ab187276) were purchased from Abcam (Tokyo, Japan). Anti-calretinin (H-45) rabbit polyclonal antibodies (sc-50453) were from Santa Cruz Biotechnology (Dallas, TX, USA). Anti-podoplanin (KS-17) rabbit polyclonal antibody was from Sigma (Saint Louis, MO, USA). The 8-hydroxy-2′-deoxyguanosine (8-OH-dG) mouse antibody (N45.1) was purchased from the Japan Institute for the Control of Aging, Nikken SEIL (Fukuroi, Japan). The anti-thromboxane synthase 1 (HPA031257) antibody was purchased from Atlas antibodies (Stockholm, Sweden).

Immunohistochemistry. Formalin-fixed paraffin-embedded tissue blocks of samples were cut to a thickness of 5 μm, placed on glass slides and deparaffinized in xylene and a graded ethanol series for 10 min. The antigen was incubated in 10 mmol/L sodium citrate buffer (pH 6.0) for 10 min in a 95°C water bath. Endogenous peroxidase activity was then blocked using 0.3% hydrogen peroxide in methanol. The slides were rinsed with TBS containing 0.1% Tween 20 and then blocked with normal goat serum for 60 min. The sections were then incubated with anti-CEA (1:100 dilution), anti-calretinin (1:50), anti-wilms tumor-1 (1:100), anti-podoplanin (1:100), anti-EpCAM (1:100), anti-8-OH-dG (1:10) and anti-TBXAS1 (1:100) antibodies overnight at 4°C. The rat sample sections were stained with anti-rabbit, anti-mouse or avidin-biotinylated HRP-conjugate antibodies according to the staining protocol (LSAB 2 System-HRP for use on rat specimens #K0609; Dako Cytomation, Tokyo, Japan), and then reacted with 3,30-diaminobenzidine. The human sample sections were stained with biotinylated anti-rabbit antibodies and avidin-biotinylated HRP conjugates for 10 min (LSAB 2 Kit Code 4002; Dako Cytomation). Finally, the sections were counterstained with hematoxylin. Two investigators (D.M. and K.K.) evaluated the immunostaining results as positive or negative in the rat samples and as positive, weakly positive or negative in the human samples. Expression in human tumor tissues was quantified using three representative cores per sample according to the staining intensity (negative, weakly positive or positive) × the percentage of cells stained (<5, <50 or <100%), as described previously by Cathcart *et al.*[12]

Array-based comparative genomic hybridization. Genomic DNA was extracted from tissue samples and purified using a QIAamp DNA blood kit (Qiagen, Tokyo, Japan). The reference DNA was extracted from tissue samples in the physiological saline solution group (group 1). Whole genome screening was performed to assess copy number variants (CNV) using a CNV-targeted oligonucleotide array based on CGH (array CGH). The Agilent SurePrint G3 Rat CGH 1× 1M Microarray (Agilent Technologies, Santa Clara, CA, USA), which includes 962 967 CNV probes, was used. The CNV array experiments were performed according to the manufacturer's instructions.[13] Briefly, test and reference genomic DNA samples (1500 ng per sample) were labeled fluorescently with Cy5 (test) and Cy3 (reference) using a ULS Labeling Kit (Agilent Technologies). For each sample, the respective labeling reactions were mixed and then separated prior to hybridization to each array. The labeled test and reference DNA samples were combined, denatured, pre-annealed with Cot-1 DNA (Thermo Fisher Scientific Inc., Waltham, MA, USA) and blocking agent, and then hybridized to the arrays for 40 h in a rotating oven at 65°C and 0.04 g (Agilent Technologies). After hybridization and washing, the arrays were scanned at a 3-μm resolution using an Agilent G2505C scanner. The images were analyzed using Feature Extraction Software 10.7.3.1 (Agilent Technologies) and the CGH 107 Sep09 protocol for background subtraction and normalization. Data from the microarray experiments were analyzed using Agilent Genomic Workbench 6.5 software and the Aberration Detection Method-2 statistical algorithm based on the combined $\log_2$ ratios at a threshold of 6. The data were centralized, and calls with mean $\log_2$ ratios <0.25 were filtered to exclude false positives.

Quantitative PCR. Quantitative PCR was performed using GeneAmp 5700 (Applied Biosystems, Tokyo, Japan). Genomic DNA was extracted and purified from rat tissue samples using a QIAamp DNA blood kit (Qiagen). The copy number ratio of *TBXAS1* to *GAPDH* was calculated using RT^2 qPCR Primer Assays for rat *Tbxas1* and *Gapdh* (catalog numbers PPR46265A and PPR06557B, respectively; Qiagen). DNA was extracted from cell lines and human clinical samples using a QIAamp DNA Mini Kit (Qiagen) and analyzed using an Hs_TBXAS1_1_SG QuantiTect Primer Assay (Catalog

Table 1. Incidence of mesothelioma induced by intraperitoneal ferric saccharate

Treatment groups (number of rats used)	Number of rats with mesothelioma
1. PSS (2)	0
2. NTA (2)	0
3. Ferric saccharate with NTA (10)	5

NTA, nitrilotriacetic acid disodiumu salt; PSS, physiological saline solution.

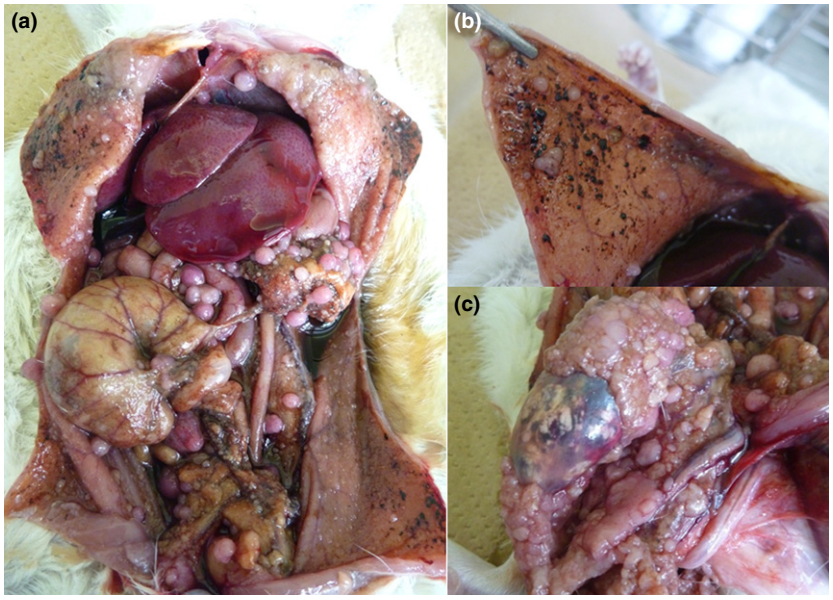

Fig. 1. Macroscopic appearance of mesothelioma in Wistar rats. (a, b) Widespread peritoneal mesotheliomas were identified in rats treated with ferric saccharate and nitrilotriacetic acid. (c) Mesothelial tumors were observed in the tunica vaginalis.

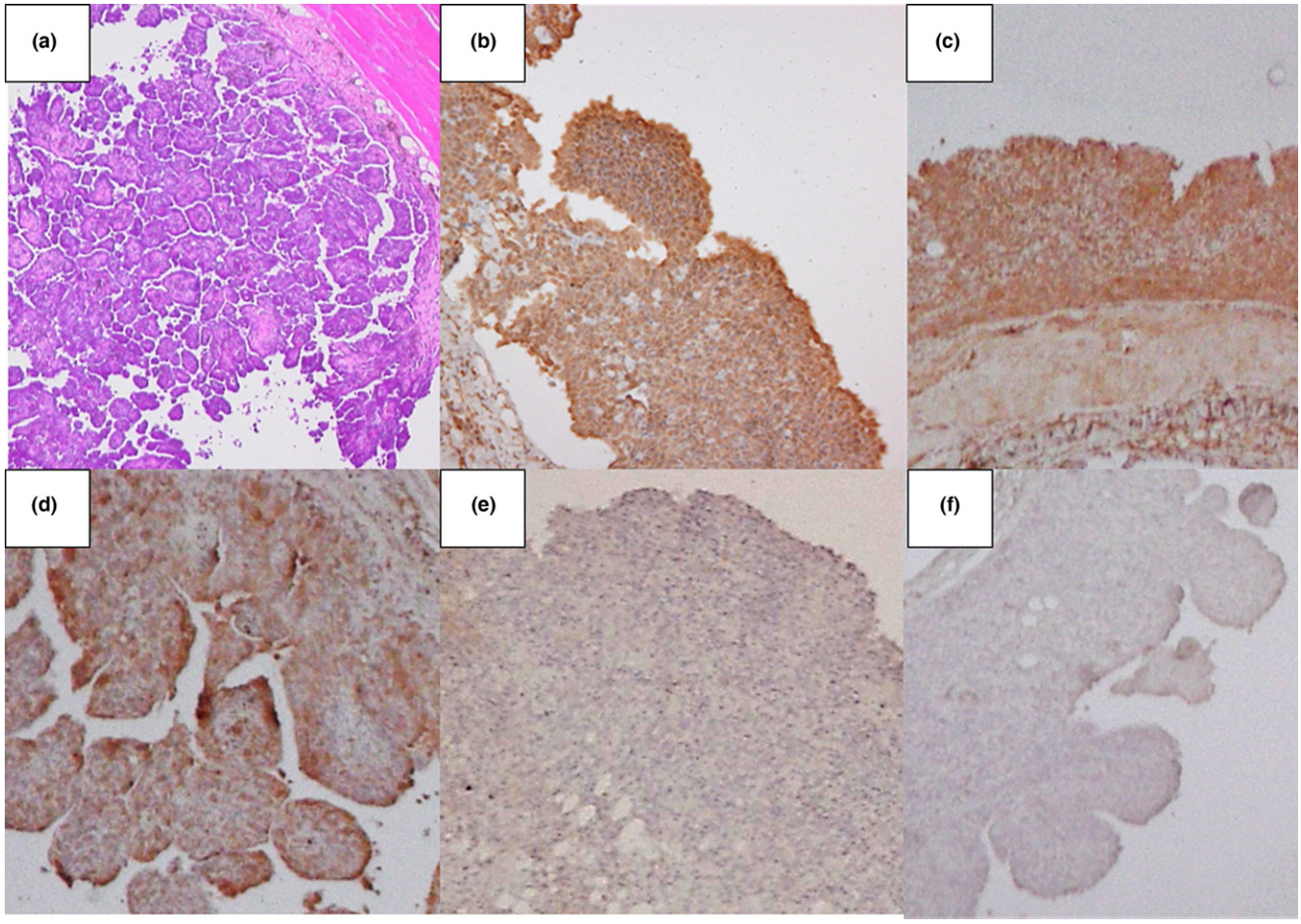

Fig. 2. Microscopic appearance of mesothelioma in Wistar rats (×40). (a) A tubulopapillary pattern was observed (H&E staining). (b) Carletinin-positive staining in the nucleus of tumor cells. (c) Wilms tumor-1 staining in the nucleus of tumor cells. (d) Podoplanin (D2-40) staining in the cytoplasm of tumor cells. (e) Negative staining for carcinoembryonic antigen. (f) Negative staining for Ep-CAM.

Number QT00090307; Qiagen). *GAPDH* forward (5′-GGCTCCCACCTTTCTCATCC-3′) and reverse (5′-GCAGCG TACTCCCCACATC-3′) primers were purchased from Sigma-Genosys.

Statistical analysis. Statistical analyses were performed using Microsoft Office Excel 2007 (Microsoft Japan Corporation, Tokyo, Japan). Comparisons between groups were made using the unpaired Student's *t*-test, and *P*-values <0.05 were considered to be statistically significant.

Results

Ferric nitrilotriacetate-induced mesothelioma model. All of the rats appeared healthy, and there were no differences in body weight among groups during treatment (data not shown). The emergence of mesothelioma was detected in only group 3 (Table 1). Five of the ten rats had widespread peritoneal mesotheliomas (M1–M5; Fig. 1a,b). Mesothelial tumors were also observed in the serosa of the tunica vaginalis of the five rats (Fig. 1c). Microscopically, they were epithelial tumors with tubule-papillary patterns (Fig. 2a). Immunohistochemical staining was performed to confirm the mesothelial lineage of the tumors (Fig. 2b, positive for calretinin; Fig. 2c positive for wilms tumor-1; Fig. 2d positive for podoplanin; Fig. 2e, negative for CEA; Fig. 2f, negative for Ep-CAM). In addition, oxidative DNA modifications were determined using immunohistochemical staining of 8-OH-dG, which stained the nuclei of mesothelioma cells (Fig. 3; Suppl. Fig. S1).

Genomic alterations in ferric nitrilotriacetate-induced mesothelioma. Array-based CGH analysis revealed a common chromosomal deletion in three of the five rats with mesothelioma (M1, M3 and M5 in Fig. 4), which was mapped to the chromosome 4q31 locus containing the *TBXAS1* gene. There were numerous other genomic amplifications and deletions, but they were not consistent among tumors. A chromosomal deletion was mapped to the chromosome 5q32 locus (containing the *Cdkn2a/b* gene), which was reported previously by Akatsuka *et al.*,[14] in one mesothelioma rat (M2) (Suppl. Table S1). The downregulation of *TBXAS1* was confirmed using quantitative PCR (Suppl. Fig. S2).

***TBXAS1* expression in cell lines and clinical samples.** The *TBXAS1* gene copy number was compared among four malignant mesothelioma cell lines and normal bronchial epithelial cells (Met5A) using quantitative PCR. *TBXAS1* gene expression was slightly but significantly reduced in three of the four mesothelioma cell lines compared with normal cells (Fig. 5). Subsequently, TBXAS1 protein expression was evaluated in clinical mesothelioma samples and compared with that in non-malignant pleural thickening. Five cases showed weakly positive staining in 10–30% of the tumor cells, and three cases showed positive staining in 70–100% of cells. Thus, out of eight mesothelioma patients, TBXAS1 staining was weakly positive in five and positive in three. The cytoplasm of non-mesothelial cells was stained negatively (Fig. 6a). The mesothelioma cells had weakly positive (Fig. 6b) and positive (Fig. 6c) stains. TBXAS1 gene expression in human malignant mesothelioma tissues (H3, H4, H6, H7 and H8) was decreased when compared with normal bronchial epithelial cells (control), although statistical significance was observed in only H4 (Suppl. Fig. S3).

Discussion

In the present study, iron-induced mesothelioma was observed in the peritoneum and the tunica vaginalis. Although the tunica vaginalis is a rare site of primary mesothelioma in humans,[15] it is a susceptible site in certain animal models.[6,16] Molecular studies have identified somatic genetic and epigenetic alterations, including those in *NF2*, *BAP1* and *CDKN2A*, in malig-

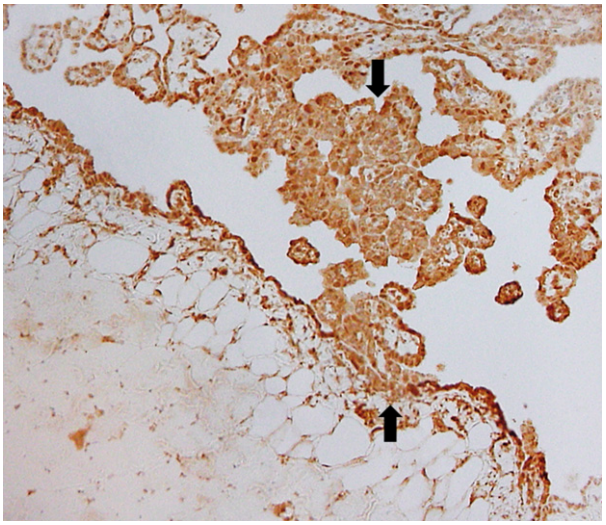

Fig. 3. Immunohistochemical analysis of the oxidized DNA base 8-hydroxy-2′-deoxyguanosine (8-OH-dG). The nuclei in mesothelioma cells on the surface of peritoneum stained positively. The tumor cells infiltrated into fat tissues (×100).

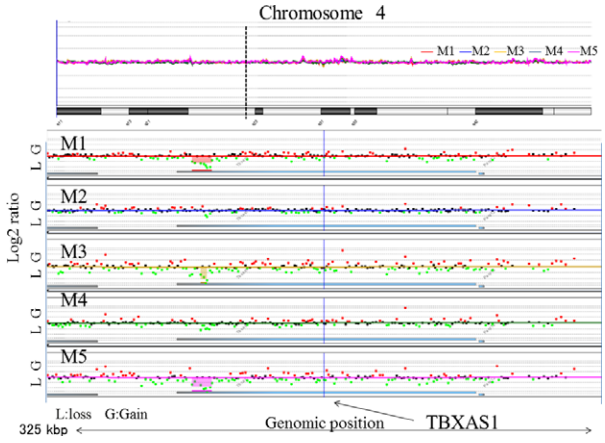

Fig. 4. Array-based comparative genomic hybridization (CGH) analysis. A common chromosomal downregulation was identified in three of five rats with mesothelioma (M1, M3 and M5), which was mapped to the chromosome 4q31 locus containing the genes encoding the *TBXAS1*.

Table 2. Genomic alternation with deletion of TBXAS1

Tumor case	Loss of copy number at TBXAS1 (log_2 ratio)
M1	−1.217
M3	−2.013
M5	−1.614

Copy number at TBXAS1 analyzed using reference DNA extracted from a normal peritoneum of a rat.

nant mesothelioma.[17] This is the first report to show that *TBXAS1* was downregulated in three of five mesothelioma rats and three of four mesothelioma cell lines. Consistent with this, *TBXAS1* expression was suppressed in five of eight human mesothelioma tissues, despite the small number of samples. MSTO-211H was the only cell line that did not show a decrease in TBXAS1 (Fig. 5). Concerning histologic types, H2052 and H290 are epithelial, H28 is sarcomatoid and MSTO-211H is biphasic. Although the difference of TBXAS1 expression might depend on the different histology, it remains unclear. More mesothelioma cell lines should be used in further study.

TBXAS1 encodes thromboxane synthase (TXAS), an enzyme in the arachidonic acid cascade that produces thromboxane A2, which plays a key role in platelet aggregation.[18] Defects in TBXAS1 cause Ghosal hematodiaphyseal dysplasia (GHDD),[19] a rare autosomal recessive disorder characterized by increased bone density with predominant diaphyseal involvement and aregenerative corticosteroid-sensitive anemia. TBXAS1 deficiency also leads to hemorrhagic diathesis.[18,20] Platelets from subjects with GHDD exhibit specific defects in arachidonic acid-produced aggregation.[20] Jiang *et al.*[21] demonstrate that the pathogenesis of chrysotile-induced mesothelial carcinogenesis is closely associated with iron overload, which is presumably due to the high hemolytic activity of chrysotile. The relationship between iron overload and hemorrhagic diathesis after TBXAS1 downregulation in the current study is compatible with Jiang's study. In breast cancer, TBXAS1 was expressed at significantly low levels in high grade tumors and in patients with poor prognosis.[22] Moreover, common single nucleotide polymorphisms or haplotypes in *TBXAS1* genes were associated with breast cancer risk.[23] Conversely, *TXAS* overexpression was observed in a variety of other cancer types, including thyroid,[24] bladder,[25] prostate,[26] lung and colorectal cancers.[27] In non-small cell lung cancer, *TXAS* overexpression was not correlated with survival.[12] The relationship between TBXAS1 expression and clinicopathological factors or survival could not be determined in the current study because of the small number of patients. Therefore, future studies evaluating *TBXAS1 in vitro* and *in vivo* might be of interest, and additional studies including a large series of patients should be performed. In the present study, five out of ten rats grew mesothelioma, but the other five rats did not. Okada *et al.*[10] also report that thirteen of nineteen rats treated with iron-NTA had mesothelioma. In contrast, asbestos fiber in the peritoneum induced all rats ($n = 26$) to grow mesothelioma.[28] Iron played a major role in catalyzing free radical production[10] and the pathogenesis of chrysotile-induced mesothelial carcinogenesis was closely associated with iron overload.[21] Although the carcinogenicity for mesothelioma in rats may presumably differ between iron-NTA and asbestos, further investigation is needed. As a limita-

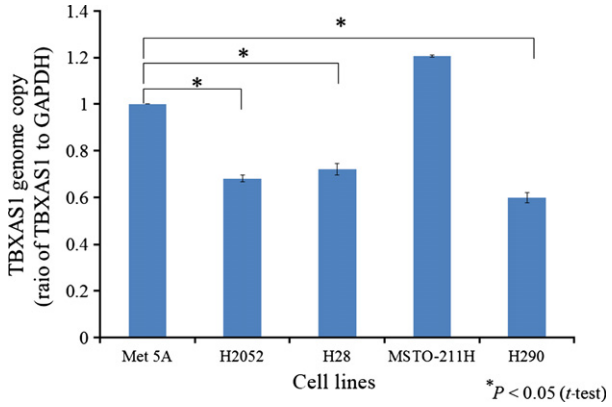

Fig. 5. Quantitative PCR. *TBXAS1* gene expression was decreased significantly in three malignant mesothelioma cell lines (H2052, H28 and H2903) compared with normal bronchial epithelial cells (Met5A). Bars, means ± SD of triplicate samples; $^*P < 0.05$ (Student's *t*-test).

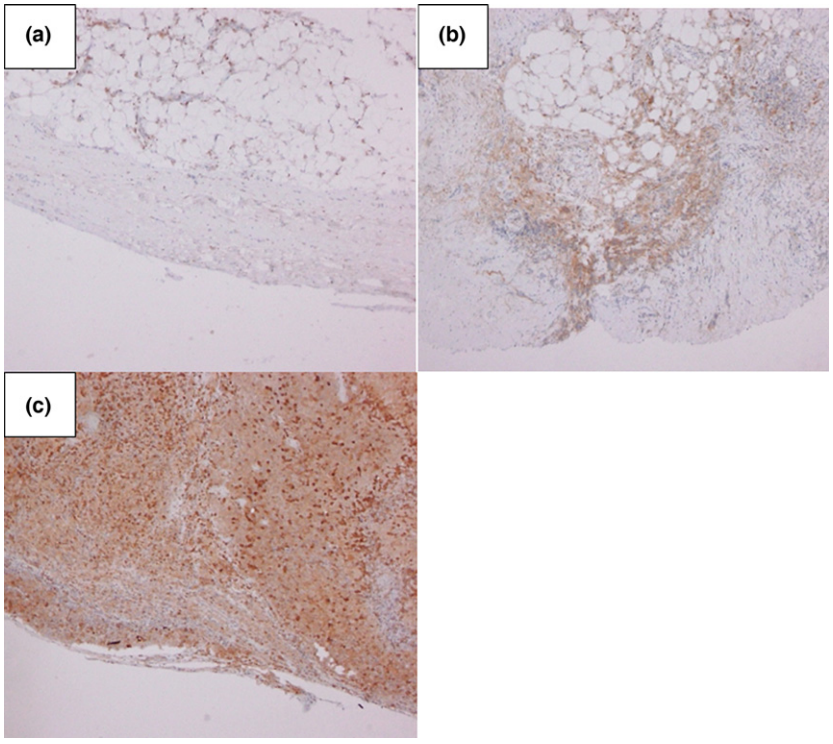

Fig. 6. Immunohistochemistry for thromboxane A synthase 1 (TBXAS1) in human malignant mesothelioma (×40). (a) The cytoplasm of non-mesothelial cells was stained negatively. Mesothelioma cells stained weakly positive (b) and positive (c).

tion of the study, we cannot refer to the relationship between asbestos and downregulation of *TBXAS1*. Future study using asbestos-induced rat mesothelioma should be performed. In addition, Hu *et al.*[29] found homozygous deletion of *CDKN2A/2B* in iron saccharate-induced mesothelioma rat model. One tumor (M2) in the present study also had the alternation and confirmed their data. The downregulation of *TBXAS1* and the homozygous deletion of *CDKN2A/2B* might be exclusive in the rat models. The relationships between their genetic alterations and overload of iron should be clarified.

Because advanced malignant mesothelioma remains difficult to cure, the malignant potential of mesothelioma needs to be suppressed. In crocidolite-induced mesothelioma in rats, deferasirox administration increased the proportion of the less malignant epithelioid subtype significantly.[30] Moreover, iron reduction could make lower risk of hepatic[31] likely other cancers.[32] Akatsuka *et al.*[14,33] demonstrate that oxidative stress caused extensive genomic alterations in the cancer genome at the chromosomal level in Fe-NTA-induced rat renal cell carcinomas. In addition, oxidative stress induced cancer following serious damage to tissues, whereas antioxidants protected against the oxidative damage.[34,35] Thus, iron depletion or antioxidant therapy might prevent the development of mesothelioma in asbestos-exposed patients.

In conclusion, *TBXAS1* gene expression was downregulated in iron-induced mesothelioma rats. The relationship between iron overload and the downregulation of *TBXAS1* should be clarified further.

Acknowledgments

This study was supported in part by Grants-in-Aid from the Ministry of Education, Culture, Sports, Science, and Technology, Japan (23659432 [K. Kiura]), by the Okayama University Center of Excellence program (K. Kiura), by a Strategic Research Foundation Grant-aided Project for Private Universities from the Ministry of Education, Culture, Sport, Science, and Technology, Japan (N. Takigawa) and by Grant-in-Aid from Novartis Pharma K.K, Japan (D.Minami). The authors thank Dr Adi F. Gazdar, Department of Pathology, University of Texas Southwestern Medical Center (Dallas, TX, USA) for providing the H2052, H28 and H290 cell lines.

Disclosure Statement

The authors have no conflict of interest to declare.

References

1 Britton M. The epidemiology of mesothelioma. *Semin Oncol* 2002; **29**: 18–25.
2 Ismail-Khan R, Robinson LA, Williams CC *et al.* Malignant pleural mesothelioma: comprehensive review. *Cancer Control* 2006; **13**: 255–63.
3 Robinson B, Lake R. Advances in malignant mesothelioma. *N Engl J Med* 2005; **353**: 1591–603.
4 de Assis LV, Locatelli J, Isoldi MC. The role of key genes and pathways involved in the tumorigenesis of malignant mesothelioma. *Biochim Biophys Acta* 2014; **1845**: 232–47.
5 Toyokuni S. Iron overload as a major targetable pathogenesis of asbestos-induced mesothelial carcinogenesis. *Redox Rep* 2014; **19**: 1–7.
6 Marques O, da Silva BM, Porto G *et al.* Iron homeostasis in breast cancer. *Cancer Lett* 2014; **28** (347): 1–14.
7 Toyokuni S. Iron-induced carcinogenesis: the role of redox regulation. *Free Radic Biol Med* 1996; **20**: 553–66.
8 Toyokuni S. Role of iron in carcinogenesis: cancer as a ferrotoxic disease. *Cancer Sci* 2009; **100**: 9–16.
9 Richimond HG. Induction of sarcoma in the rat by iron-dextran complex. *Br Med J* 1959; **1**: 947–9.
10 Okada S, Hamazaki S, Toyokuni S *et al.* Induction of mesothelioma by intraperitoneal injections of ferric saccharate in male wistar rats. *Br J Cancer* 1989; **60**: 708–11.
11 Ke Y, Reddel RR, Gerwin BI *et al.* Establishment of a human in vitro mesothelial cell model system for investigating mechanisms of asbestos-induced mesothelioma. *Am J Pathol* 1989; **134**: 979–91.
12 Cathcart MC, Gately K, Cummins R *et al.* Examination of thromboxane synthase as a prognostic factor and therapeutic target in non-small cell lung cancer. *Mol Cancer* 2011; **10**: 25.
13 de Smith AJ, Tsalenko A, Sampas N *et al.* Array CGH analysis of copy number variation identifies 1284 new genes variant in healthy white males: implications for association studies of complex diseases. *Hum Mol Genet* 2007; **16**: 2783–94.
14 Akatsuka S, Yamashita Y, Ohara H *et al.* Fenton reaction induced cancer in wild type rats recapitulates genomic alterations observed in human cancer. *PLoS One* 2012; **7**: e43403.
15 Amthor M, Falk S, Tuma F *et al.* Das malignediffuse mesotheliom der Hodenhullen, Bericht uber einen Fall mitimmunohistochemischer Auswertung. *Pathologe* 1998; **9**: 55–8.
16 Cabral JRP, Neal GE. Testicular mesotheliomas in rats exposed to N-2-fluorenylacetamide (FAA). *Tumori* 1983; **69**: 195–9.
17 Sekido Y. Molecular pathogenesis of malignant mesothelioma. *Carcinogenesis* 2013; **34**: 1413–9.
18 Shen RF, Tai HH. Thromboxanes: synthase and receptors. *J Biomed Sci* 1998; **5**: 153–72.
19 Ghosal SP, Mukherjee AK, Mukherjee D *et al.* Diaphyseal dysplasia associated with anemia. *J Pediatr* 1988; **113**: 49–57.
20 Geneviève D, Proulle V, Isidor B *et al.* Thromboxane synthase mutations in an increased bone density disorder (Ghosal syndrome). *Nat Genet* 2008; **40**: 284–6.
21 Jiang L, Akatsuka S, Nagai H *et al.* Iron overload signature in chrysotile-induced malignant mesothelioma. *J Pathol* 2012; **228**: 366–77.
22 Watkins G, Douglas-Jones A, Mansel RE *et al.* Expression of thromboxane synthase, TBXAS1 and the thromboxane A2 receptor, TBXA2R, in human breast cancer. *Int Semin Surg Oncol* 2005; **2**: 23.
23 Abraham JE, Harrington P, Driver KE *et al.* Common polymorphisms in the prostaglandin pathway genes and their association with breast cancer susceptibility and survival. *Clin Cancer Res* 2009; **15**: 2181–91.
24 Kajita S, Ruebel KH, Casey MB *et al.* Role of COX-2, thromboxane A2 synthase, and prostaglandin I2 synthase in papillary thyroid carcinoma growth. *Mod Pathol* 2005; **18**: 221–7.
25 Moussa O, Yordy JS, Abol-Enein H *et al.* Prognostic and functional significance of thromboxane synthase gene overexpression in invasive bladder cancer. *Cancer Res* 2005; **65**: 11581–7.
26 Nie D, Che M, Zacharek A *et al.* Differential expression of thromboxane synthase in prostate carcinoma: role in tumour cell motility. *Am J Pathol* 2004; **164**: 429–39.
27 Nie D, Lamberti M, Zacharek A *et al.* Thromboxane A (2) regulation of endothelial cell migration, angiogenesis, and tumour metastasis. *Biochem Biophys Res Commun* 2000; **267**: 245–51.
28 Okazaki Y, Nagai H, Chew SH *et al.* CD146 and insulin-like growth factor 2 mRNA-binding protein 3 predict prognosis of asbestos-induced rat mesothelioma. *Cancer Sci* 2013; **104**: 989–95.
29 Hu Q, Akatsuka S, Yamashita Y *et al.* Homozygous deletion of CDKN2A/2B is a hallmark of iron-induced high-grade rat mesothelioma. *Lab Invest* 2010; **90**: 360–73.
30 Nagai H, Okazaki Y, Chew SH *et al.* Deferasirox induces mesenchymal–epithelial transition in crocidolite-induced mesothelial carcinogenesis in rats. *Cancer Prev Res (Phila)* 2013; **6**: 1222–30.
31 Kato J, Miyanishi K, Kobune M *et al.* Long-term phlebotomy with low-iron diet therapy lowers risk of development of hepatocellular carcinoma from chronic hepatitis C. *J Gastroenterol* 2007; **42**: 830–6.
32 Zacharski LR, Chow BK, Howes PS *et al.* Decreased cancer risk after iron reduction in patients with peripheral arterial disease: results from a randomized trial. *J Natl Cancer Inst* 2008; **100**: 996–1002.
33 Toyokuni S, Akatsuka S. What has been learned from the studies of oxidative stress-induced carcinogenesis: proposal of the concept of oxygenomics. *J Clin Biochem Nutr* 2006; **39**: 3–10.
34 Ohsawa I, Ishikawa M, Takahashi K *et al.* Hydrogen acts as a therapeutic antioxidant by selectively reducing cytotoxic oxygen radicals. *Nat Med* 2007; **13**: 688–94.
35 Tanaka K, Azuma A, Miyazaki Y *et al.* Effects of lecithinized superoxide dismutase and/or pirfenidone against bleomycin-induced pulmonary fibrosis. *Chest* 2012; **142**: 1011–9.

Supporting Information

Additional supporting information may be found in the online version of this article:

Fig. S1. Immunohistochemical analysis of the oxidized DNA marker 8-hydroxy-2′-deoxyguanosine (8-OH-dG). The nuclei of mesothelial cells on the surface of the peritoneum in groups 1 (a) and 2 (b) were stained negatively (×40).

Fig. S2. Quantitative PCR. *TBXAS1* expression was decreased significantly in rats with Fe-NTA-induced malignant mesothelioma (M1, M3 and M5). Bars, means ± SD in triplicate; $*P < 0.05$ (Student's *t*-test).

Fig. S3. Quantitative PCR. *TBXAS1* gene expression in human malignant mesothelioma tissues (H3, H4, H6, H7 and H8) was decreased when compared with normal bronchial epithelial cells (control), although the statistical significance was observed in only H4. Bars, means ± SD of triplicate samples; $*P < 0.05$ (Student's *t*-test).

Table S1. Genomic alternation with deletion of Cdkn2a/b. Copy number at Cdkn2a/b analyzed using reference DNA extracted from a normal peritoneum of a rat.